Deregulated Splicing Is a Major Mechanism of RNA-Induced Toxicity in Huntington's Disease

Judith Schilling[1], Meike Broemer[1], Ilian Atanassov[2], Yvonne Duernberger[1], Ina Vorberg[1,3], Christoph Dieterich[2], Alina Dagane[4], Gunnar Dittmar[4,5], Erich Wanker[4], Willeke van Roon-Mom[6], Jennifer Winter[7] and Sybille Krauß[1]

1 - German Center for Neurodegenerative Diseases (DZNE), *53127, Bonn, North Rhine-Westphalia, Germany*
2 - Max Planck Institute for Biology of Ageing, *50931 Cologne, North Rhine-Westphalia, Germany*
3 - Department of Neurology, *Friedrich-Wilhelms-Universität Bonn, 53127 Bonn, North Rhine-Westphalia, Germany*
4 - Max-Delbrück-Center for Molecular Medicine (MDC), *13092 Berlin, Germany*
5 - Luxembourg Institute of Health, *1445 Strassen, Luxembourg*
6 - Leiden University Medical Center, *2333, ZC, Leiden, the Netherlands*
7 - Institute of Human Genetics, *University Medical Center, Johannes Gutenberg University Mainz, 55131 Mainz, Rhineland-Palatinate, Germany*

Correspondence to Sybille Krauß: *Miltenyi Biotec GmbH, Friedrich-Ebert-Straße 68, 51429 Bergisch Gladbach, Germany. krauss.sybille@gmx.de*
https://doi.org/10.1016/j.jmb.2019.01.034
Edited by Kristine Karla Freude

Abstract

Huntington's disease (HD) is caused by an expanded CAG repeat in the huntingtin (*HTT*) gene, translating into an elongated polyglutamine stretch. In addition to the neurotoxic mutant HTT protein, the mutant CAG repeat RNA can exert toxic functions by trapping RNA-binding proteins. While few examples of proteins that aberrantly bind to mutant *HTT* RNA and execute abnormal function in conjunction with the CAG repeat RNA have been described, an unbiased approach to identify the interactome of mutant *HTT* RNA is missing. Here, we describe the analysis of proteins that preferentially bind mutant *HTT* RNA using a mass spectrometry approach. We show that (I) the majority of proteins captured by mutant *HTT* RNA belong to the spliceosome pathway, (II) expression of mutant CAG repeat RNA induces mis-splicing in a HD cell model, (III) overexpression of one of the splice factors trapped by mutant *HTT* ameliorates the HD phenotype in a fly model and (VI) deregulated splicing occurs in human HD brain. Our data suggest that deregulated splicing is a prominent mechanism of RNA-induced toxicity in HD.

Huntington's disease (HD) is caused by an expanded CAG repeat motif in the huntingtin (*HTT*) gene, translating into an elongated polyglutamine stretch in the HTT protein. The pathological hallmark of HD is aggregation of mutant HTT protein in patient brains [1]. These aggregates are enriched in truncated HTT protein species that are either generated by several proteases or are a result of an aberrantly spliced exon1-transcript and contain the polyglutamine stretch. Aggregate-prone HTT proteins play a crucial role in disease pathology, but it is still unclear if the aggregates or folding intermediates thereof represent the toxic species. Hence, it seems that there are multiple mechanisms that each contributes a little bit to toxicity [2–6].

A growing body of evidence argues that, in addition to aggregate-prone proteins, the CAG repeat mRNA itself contributes to neurotoxicity in CAG repeat expansion disorders. Mechanistically, this likely involves a gain-of-function at the RNA level [7,8]. Mutant *HTT* mRNA differs structurally from mRNA with physiological CAG repeat lengths. While *HTT* transcripts with non-disease causing numbers of repeats exhibit either a very short or no CAG repeat hairpin structure, in transcripts with disease-associated numbers of repeats, a CAG hairpin is present and extended from a three-helix junction [9,10]. Aberrant binding of proteins to these pathological RNA structures may lead to aberrant functions of such

RNA–protein complexes and may contribute to HD pathogenesis [8,11].

Several examples of RNA-binding proteins that are trapped by mutant *HTT* RNA have been published to date. For example, the splicing factor muscleblind 1 (MBNL1) co-localizes with the mutant CAG repeat RNA, and as a result, the splicing patterns of known MBNL1 target mRNAs are altered in cell models and in HD patient cells [12]. Another example is the endonuclease DICER that is an essential component of the siRNA machinery. In cell models as well as mouse models of HD, the mutant CAG repeat RNA is cleaved by DICER into 21-nt-long small CAG-repeated RNAs (sCAGs), which are able to bind to CTG repeat containing genes through the RNA interference machinery. Consequently, this leads to deregulated expression of CTG repeat containing genes [13]. Furthermore, proteins that are trapped by mutant *HTT* RNA are translational regulators that functionally induce translation of mutant polyglutamine protein upon binding, like the ubiquitin ligase MID1 [14]. These results suggest that there will be more RNA-binding proteins similarly recruited to mutant *HTT* mRNA and exert abnormal function und thus could contribute to HD pathology.

In this study, we investigated in an unbiased experimental approach which proteins are captured by *HTT* RNA in a CAG repeat length-dependent manner. Our data show that the majority of proteins that are sequestered by mutant *HTT* RNA belong to the spliceosome pathway. In line with this observation we show that expression of mutant *HTT* induces mis-splicing in an HD cell model. Furthermore, we show that overexpression of one of the splice factors trapped by mutant *HTT* rescues the toxic phenotype in an HD fly model. Finally, we show that deregulated splicing occurs in human HD brain. Our data suggest that deregulated splicing is a major mechanism of RNA-induced toxicity in HD.

Mutant *HTT* RNA captures proteins that belong to the splicing pathway

To identify proteins that are captured by mutant *HTT* exon 1 (ex1) RNA and may be involved in RNA-mediated neurotoxicity, we performed an RNA–protein binding experiment using *in vitro* transcribed *HTT*ex1 RNAs containing wild-type or mutant CAG repeats immobilized on magnetic beads as baits. After incubation with cell extracts to allow RNA–protein binding, beads were washed and RNA-bound proteins were eluted and analyzed by quantitative mass spectrometry. By this approach, we identified 134 proteins that specifically bound to *HTT*ex1 RNA (Supplementary Fig. 1). Thirty-six of these proteins bound in a length-dependent manner with a higher affinity for RNAs harboring mutant CAG repeats. The majority of these 36 proteins belong to the splicing pathway (Fig. 1a/b, Supplementary Fig. 2, Supplementary Table 1). Splicing of nascent precursor messenger RNA (pre-mRNA) molecules to remove introns and link exons is carried out by the spliceosome that consists of several proteins and small nuclear RNAs. The major spliceosome comprises the small nuclear ribonucleoproteins (snRNPs) U1, U2, U4, U5 and U6. Stepwise sequential assembly of these snRNPs on the pre-mRNA executes splicing reactions. Splicing starts with U1 attaching to a specific sequence at the 5′ splice site of an exon. At the same time, U2 assembles at the branch site upstream of the 3′ splice site of the downstream exon, forming the prespliceosome. Binding of the U5 and U4–U6 complexes to the prespliceosome results in formation of the precatalytic spliceosome. By unwinding of the U4–U6 complexes, U4 and U1 are released from the prespliceosomal complex. The 5′ splice site gets cleaved, a looped structure, called lariat, is removed and the two exons are covalently linked [15,16]. Interestingly, the 36 identified proteins that bind *HTT* RNA in a CAG repeat length-dependent manner include proteins of all snRNPs, U1, U2, U4, U5 and U6. Among the identified proteins is SRSF6, a known mutant *HTT* RNA interactor [17]. Furthermore, the identified proteins include PRPF8, a splicing factor that is linked to polyglutamine-mediated toxicity [18], as well as to the pathogenesis of retinitis pigmentosa, a progressive neurodegenerative disease [19]. To validate the mass spectrometry data, we repeated the RNA–protein binding experiment and detected all four splicing factors tested, including the U5 subunit PRPF8, by Western blot (Fig. 1c).

Expression of mutant *HTT* induces mis-splicing

Aberrant binding of the identified splicing factors to mutant RNA may result in a loss of their physiological functions. To test this, we generated an SH-SY5Y cell line expressing *HTT* exon1 with 68 CAG repeats fused to GFP under an inducible promoter (see Materials and Methods for details). We then analyzed the splicing pattern of induced *versus* uninduced cells on a splicing microarray. Several mis-splicing events were detected upon expression of mutant *HTT*ex1 including retained introns (20), alternative splice acceptor (22) and splice donor (10) sites, and cassette exons (42) (Fig. 2a). Sequestration of the splice factors identified in Fig. 1 by mutant *HTT* RNA is likely the reason for these identified mis-splicing events. To validate this, we focused on PRPF8 for further analysis. PRPF8 is important for recognizing weak 5′ splice sites [20]. Supporting the idea that PRPF8 may be involved in

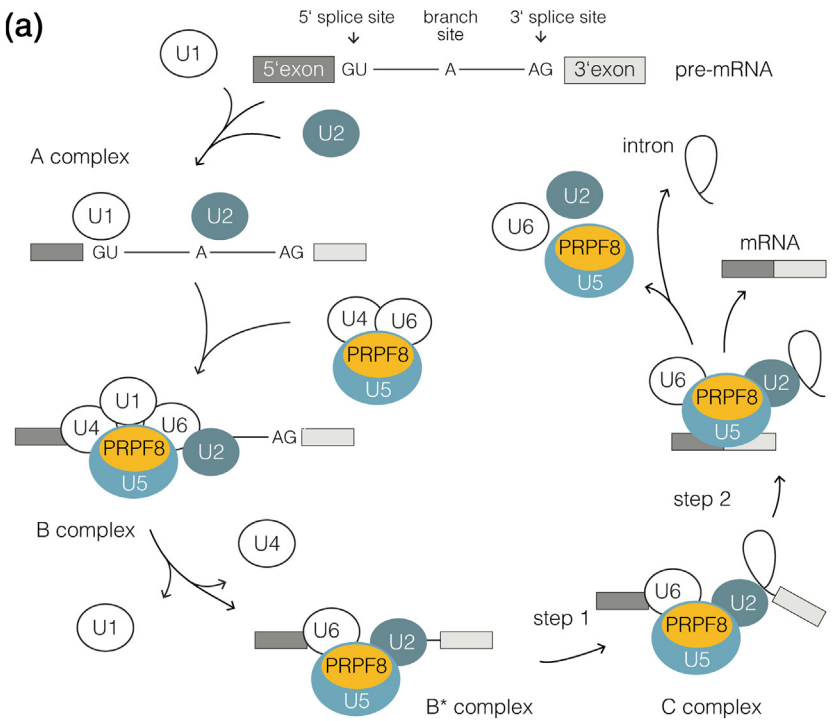

(b)

Gene	Entrez ID	Spliceosome
DDX46	9879	U2
SF3A1	10291	U2
SF3A3	10946	U2
SF3B1	23451	U2
SF3B2	10992	U2
SF3B3	23450	U2
SF3B4	10262	U2
DHX15	1665	U2 related
PUF60	22827	U2 related
U2AF2	11338	U2 related
U2SURP	23350	U2 related
EFTUD2	9343	U5
PRPF8	10594	U5
SNRNP200	23020	U5
SNRNP40	9410	U5

Gene	Entrez ID	Spliceosome
HNRNPC	3183	common
HNRNPUL2	221092	common
SRSF1	6426	common
SRSF3	6428	common
SRSF6	6431	common
TRA2B	6434	common
SNRPD1	6632	common
PRPF40A	55660	U1 related
RBM25	58517	U1 related
PRPF31	26121	U4/U6
BCLAF1	9774	complex B/C
RALY	22913	complex B/C
SON	6651	complex B/C
SRRM2	23524	complex C
EIF4A3	9775	EJC
PNN	5411	EJC
PRPF19	27339	PRP19 complex

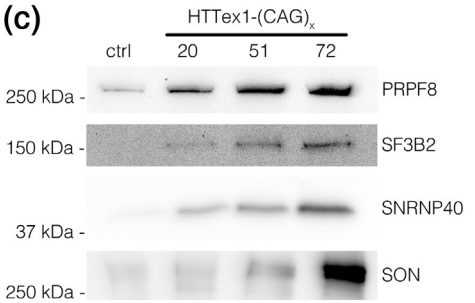

Fig. 1. Proteins that aberrantly bind mutant *HTT*ex1 RNA are associated with splicing. (a) Schematic showing the splicing cycle. PRPF8, a U5-subunit, is indicated in yellow. (b) *HTT* RNA-binding proteins were identified by RNA–protein pull-down followed by mass spectrometry. Mutant *HTT* RNA-interacting proteins (36 proteins binding in a length-dependent manner) are significantly enriched for splicing factors (see also Supplementary Figs. 1, 2, 3, and Supplementary Table 1). A list of these proteins is shown. (c) RNA–protein pull-downs of *HTT*ex1 RNA with different repeat lengths analyzed on Western blot detecting the splice factors PRPF8, SF3B2, SNRNP40 and SON. PRPF8 and SNRNP40 are components of the U5 snRNP, SF3B3 is a component of the U2 snRNP. SON probably acts by facilitating the interaction between SRSF2 and the RNA polymerase II, which is required for formation of the earliest ATP-dependent splicing complex and for interactions of U1 and U2 snRNPs with pre-mRNA.

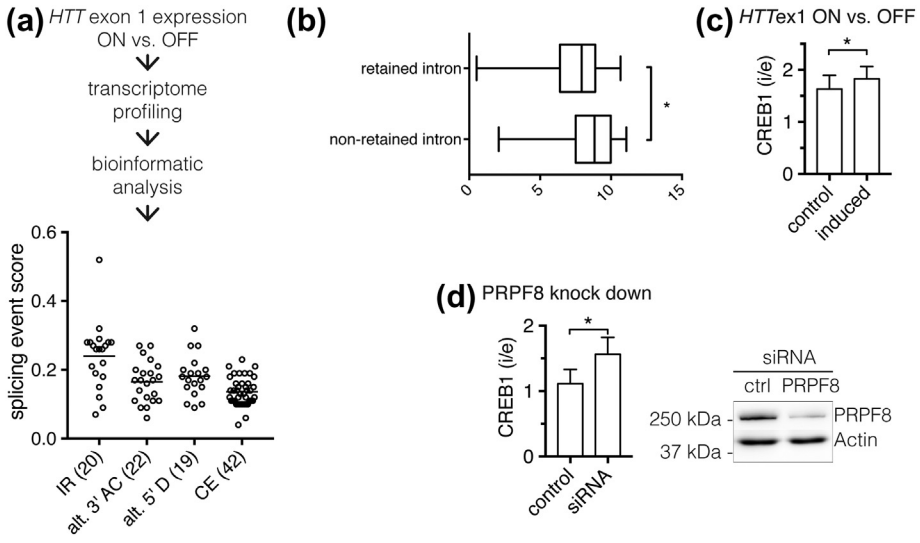

Fig. 2. *CREB1* is mis-spliced in an HD cell model and HD patients. (a) RNA of an SH-SY5Y cell model inducibly expressing GFP-*HTT*ex1(68CAG) was analyzed on a splicing microarray. Splicing patterns of uninduced controls and induced cells expressing GFP-*HTT*ex1(68CAG) were compared. The types and numbers of alternative splicing events with corresponding splicing event score detected upon expression of GFP-*HTT*ex1(68CAG) are shown. IR (intron retention), alt. 3′ AC (alternative 3′ acceptor), alt. 5′ D (alternative 5′ donor), CE (cassette exon). (b) Box plot of 5′ splice site strengths of retained introns compared to non-retained introns, mean values ± SEM, $^*p < 0.05$. (c) qRT-PCR validation of the *CREB1* IR event in SH-SY5Y-GFP-*HTT*ex1 (68CAG) cells described in panel a. Columns represent mean values ± SEM, $^*p < 0.05$, n = 7 replicate experiments using different passages of cells. *p* value is the result of a factorial ANOVA determining the effect of GFP-*HTT*ex1(68CAG) expression and correcting for *CREB1* exon expression and a confounding effect of the qPCR experiments. (d) *CREB1* IR event measured by qRT-PCR after PRPF8 knockdown in uninduced SH-SY5Y-GFP-*HTT*ex1(68CAG) cells, $^*p < 0.05$, n = 4 replicate experiments using different passages of cells. Columns represent mean values ± SEM; *p* value is the result of a factorial ANOVA determining the knockdown effect and correcting for *CREB1* exon expression and a confounding effect of the qPCR experiments. In addition, a Western blot controlling knockdown efficiency is shown.

the observed intron retention (IR) events that occur upon mutant *HTT* expression, an *in silico* analysis of splice site strengths showed that retained introns had significantly weaker 5′ splice sites than properly spliced introns (Fig. 2b).

PRPF8 regulates splicing of *CREB1*

Prompted by the above-mentioned experiments showing that splice factors including PRPF8 get trapped by mutant *HTT* RNA and that expression of mutant *HTT* RNA induces mis-splicing, we wanted to validate that depletion of PRPF8 indeed induces intron retention. Since out of the identified IR-RNAs *CREB1* has been previously linked to HD [21–24], we focused on *CREB1* for further analysis. First, we validated the intron retention event in *CREB1* after expression of mutant *HTT*ex1 RNA by quantitative (q)RT-PCR (Fig. 2c). Second, to test if depletion of PRPF8 indeed leads to mis-splicing of *CREB1*, we performed a PRPF8 knock down experiment (Fig. 2d). As expected, depletion of PRPF8 resulted in increased intron retention in the *CREB1* transcript. These data support the idea that capturing of PRPF8 by mutant *HTT* RNA, and thus, its removal from its endogenous targets like *CREB1* RNA results in their missplicing.

Overexpression of PrP8 rescues the HD phenotype

The above-mentioned experiments demonstrate that splice factors including PRPF8 get trapped by mutant *HTT* RNA, suggesting that they are thereby functionally impaired leading to mis-splicing. This deregulated splicing may be a molecular mechanism underlying toxicity of mutant CAG repeat RNA. Thus, overexpression of splice factors like PRPF8 should ameliorate the HD phenotype. To test this hypothesis, we used an established *Drosophila* model for HD that expresses mutant human *HTT*ex1 with 97 CAG repeats under the control of the eye-specific GMR-Gal4 driver, inducing loss of pigment cells [25]. Strikingly, co-expression of the PRPF8 homolog Prp8 improved the eye phenotype, supporting our finding that mis-splicing is a molecular mechanism underlying toxicity of mutant CAG repeat RNA (Fig. 3a, b). Of note, we suppose that co-expression of further splicing factors would further suppress HTT polyQ toxicity in the fly eye.

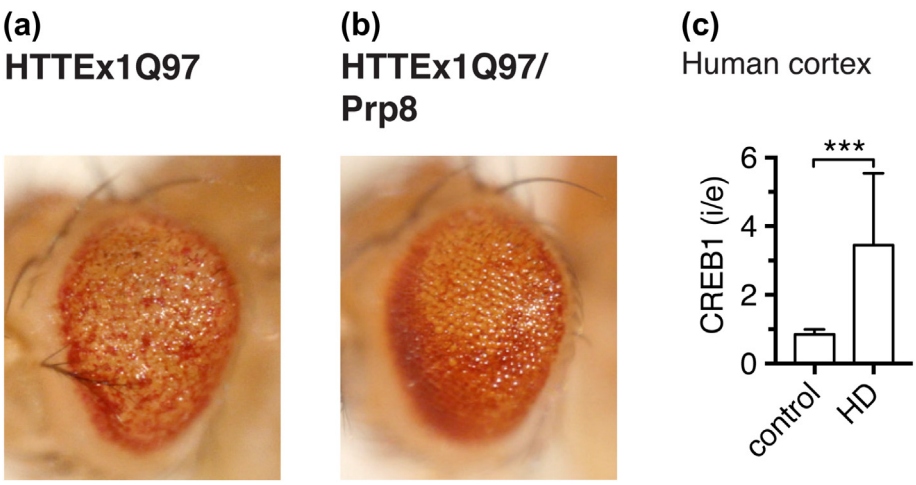

Fig. 3. Missplicing is an HD disease mechanism. (a) Expression of *HTTex1* (CAG97) leads to death of pigment cells (red) and a rough eye phenotype in *Drosophila*. (b) Co-expression of Prp8 ameliorates HTTex1-induced toxicity and partially suppresses degeneration, as shown by fewer white patches and a more even eye appearance. Pictured are eyes of male flies, 5 days old, raised at 27 °C. Genotypes: (a) GMR-Gal4/+; UAS-HttEx1Q97/+ (b) GMR-Gal4/+; UAS-HttEx1Q97/UAS-flag-Prp8. (c) *CREB1* IR event measured by qRT-PCR in human cortical tissue from unaffected individuals and HD patients. $^{**}p < 0.001$, $n_{control} = 6$, $n_{HD} = 8$; *p* value is the result of a factorial ANOVA determining the genotype effect and correcting for *CREB1* exon expression and a confounding effect of the qPCR experiments.

CREB1 is mis-spliced in HD brains

Finally, to test if mis-splicing also occurs in human HD brain, we detected IR in *CREB1* transcripts by qRT-PCR in human brain samples of HD patients and controls. Strikingly, we observed a significant increase in *CREB1* intron retention in brain tissue of HD patients (Fig. 3c).

To conclude, we present here an unbiased experimental approach to identify proteins that are captured by mutant *HTT*ex1 RNA. The majority of these proteins are splicing factors and their capturing results in deregulated splicing of several RNAs including *CREB1*. Our findings corroborate previously shown deregulated CREB1 function in neurodegenerative phenotypes and HD [21–24]. In addition, this recruitment of splicing factors supports the previous observation that mutant *HTT* RNA sequesters splicing factors such as SRSF6 (also identified here), which induces missplicing of *HTT* transcript itself [17,26]. Our findings are substantiated by a recent study describing extensive mis-splicing in HD brains [27]. Our results encourage further development of RNA-targeting strategies to inhibit aberrant RNA–protein interactions and thus stop mechanisms of RNA-induced toxicity in HD.

Materials and Methods

RNA pull-down

HTT exon 1 with varying CAG-repeat lengths was PCR amplified using GoTaq® Green Master Mix (Promega). The forward primer contains the T7 phage promotor sequence to facilitate *in vitro* RNA synthesis by T7 RNA polymerase. The purified PCR product was subjected to *in vitro* transcription using the T7 RiboMAX™ Express Large Scale RNA Production System (Promega) with addition 0.5 mM biotin-UTP (Thermo Fisher Scientific, AM8450). Biotinylated RNA was purified and folded in RNA structure buffer [10 mM Tris (pH 7), 100 mM KCl, 10 mM $MgCl_2$] by incubation at 72 °C, 10 min, followed by cooling to room temperature. Forty microliters of Dynabeads® M-280 Streptavidin (Thermo Fisher Scientific) per sample was incubated with 40 pmol of biotinylated RNA in TKM buffer [20 mM Tris, 100 mM KCl, 5 mM $MgCl_2$, 1 mM DTT, 1% NP40, complete protease inhibitor (Sigma-Aldrich), RiboLock RNase Inhibitor (Thermo Fisher Scientific)] for 30 min at room temperature. As a control, beads were coated with a mix of dNTPs and bUTPs. The coated beads were washed twice with TKM buffer. For protein lysates, four 150-cm^2 flasks of almost confluent SH-SY5Y cells were harvested and pooled. The cell pellet was lysed in 1 ml TKM buffer, homogenized using Precellys®24 Homogenizer (Peqlab), and centrifuged for 10 min at 12,000*g* and 4 °C. One milligram of protein lysate was added to the RNA coated magnetic beads at a final volume of 400 µl TKM buffer. The samples were incubated overnight at 4 °C. The beads were washed three times, and beads were resuspended in 20 µl 1 × SDS-PAGE sample buffer [50 mM Tris–Cl (pH 6.8), 100 mM DTT, 2% SDS, 0.1% bromophenol blue, 10% glycerol]. After incubation at 95 °C for 10 min, the eluted proteins were processed

for either Western blot or mass spectrometry analysis. For mass spectrometry analysis, the experiment was repeated five times on different days using different preparations of RNA and cell lysates.

Mass spectrometry and data analysis

The eluted proteins were concentrated into one band on an SDS-PAGE gel. The band was excised, and the proteins were processed using an automated sample preparation setup [28]. The generated peptides were purified on StageTips [29]. The samples were measured on a Q-Exactive mass spectrometer (Thermo-Fisher) coupled to a Proxeon nano-LC system (Thermo-Fisher) in data-dependent acquisition mode, selecting the top 10 peaks for HCD fragmentation. A 1-h gradient (solvent A: 5% acetonitrile, 0.1% formic acid; solvent B: 80% acetonitrile, 0.1% formic acid) was applied for the samples using an in-house prepared nano-LC column (0.075 mm × 150 mm, 3 µm Reprosil C18; Dr. Maisch GmbH). A volume of 2 µl sample was injected, and the peptides were eluted with 3 h gradients of 5% to 75% solvent B at flow rates of 0.25 µl/min. MS acquisition was performed at a resolution of 70,000 in the scan range from 300 to 1700 m/z. The normalized collision energy was set to 26 eV. The mass window for precursor ion selection was set to 2.0 m/z. The recorded spectra were analyzed using the MaxQuant software package (Version 1.3.0.5) [30] by matching the data to the Uniprot human database (downloaded on 06.05.2012) with a false discovery rate of 1%.

Proteomic data analysis was performed using the Perseus computational platform [31] (version 1.5.0.0) and R [32] (version 3.3). The results in ProteinGroups.txt were filtered by removing all entries corresponding to "Reverse," "Contaminant" or "Only identified by site." Next, the protein LFQ intensity values were log2 transformed and filtered for at least four valid values in at least one group (C, H20, H51 or H72). The missing values were imputed from a normal distribution with a width of 0.3 and a down shift of 1.8. Proteins, binding in a length-dependent manner, were identified with limma [33] (version 3.30.13) using a two-pass approach. First, proteins that were significantly enriched by the CAG repeats were identified using a contrast that compares the average LFQ protein intensity across the CAG repeats against the control. Second, the subset of significantly enriched proteins (adjusted p value <0.01) was analyzed using a three-way, pairwise comparison of the difference in LFQ intensity between a CAG repeat and the control. The p values of the three comparisons were corrected for multiple testing using limma's decide Tests function; the method argument was set to "global," and the adjust method argument was set to "BH." The proteins showing positive, significant difference in at least one comparison while not showing a negative, significant difference in any of the comparisons were designated as binding in a length-dependent manner.

For Gene Ontology Analysis of proteins, binding CAG length-dependently ToppGene Suite was used [34]. Proteins annotated with terms associated with splicing were manually mapped to the specific spliceosomal complexes [35].

Generation of stable cell line

To generate cell lines expressing Q68-GFP upon tetracyclin induction, we used the Lenti-X Tet-On 3G Inducible Expression System (Clontech Laboratories). *HTT* exon1 with 68 CAG repeats fused to GFP was cloned in the inducible expression vector pLVX TRE3G. To generate lentiviral particles encoding the gene of interest, HEK293/T cells were transfected with the expression vector and Lenti-X Packaging mix (VSV-G). For all steps, cells were grown under tetracycline-free conditions. Lentiviral particles were collected 48 and 72 h post-transfection, pooled and concentrated using PEG precipitation. Lentiviral particles were resuspended in PBS and stored at −80 °C. For transduction, SH-SY5Y cells were incubated with lentiviral particles in DMEM supplemented with 5% FBS and 8 µg/ml polybrene. The following day, the medium was exchanged with DMEM, 10% FBS and 5% Pen/Strep. Aliquots of the generated stable cell lines were frozen in liquid nitrogen for future experiments.

Microarray analysis

The splicing sensitive human Clariom D assay (Affymetrix, Thermo Fisher Scientific Inc.) was used to analyze differential splicing events between control and CAG 68 expressing SH-SY5Y cells. The human Clariom D assay covers the whole transcribed genome including all known splice variants (coding and non-coding). The GeneChip WT PLUS Reagent Kit (Affymetrix, Thermo Fisher Scientific Inc.) was used to generate biotinylated sense-strand cDNA of the whole transcriptome from 100 ng of total RNA from three biological replicates. Array processing was performed using the Affymetrix GeneChip Hybridization, Wash and Stain kit. cDNA was hybridized to human Clariom D arrays for 16 h in a 45 °C incubator with 60-rpm rotation. After washing and staining using the Fluidics Station 450, the microarrays were scanned with the Affymetrix GeneChip Scanner 3000, according to the manufacturer's instructions.

The data were analyzed with the Transcriptome Analysis Console (TAC) 3.1 and Expression Console 1.4 software from Affymetrix (Affymetrix, Thermo Fisher Scientific Inc.). Exons with $\geq$2-fold-change and $p < 0.05$ were selected as being significantly differentially expressed.

Analysis of splice site strengths

We used the MaxEntScan algorithm [36] to compare splice site strengths of retained to non-retained introns.

siRNA transfection

SH-SY5Y cells were seeded in 24-well plates (10^5 cell/well) 1 day prior to transfection. The PRPF8 siRNAs (GeneSolution Cat. No. 1027416, Gene ID: 10594; Qiagen) were pooled to a final concentration of 20 μM. As a negative control, a non-silencing siRNA (AATTCTCCGAACGTGTCACGT) was used. siRNA cocktail (2.5 μl) per well was transfected using Lipofectamine 2000 (Thermo Fisher Scientific) according to the manufacturer's instructions.

Western blot

Protein extracts were dissolved in SDS-PAGE sample buffer and boiled 10 min at 95 °C, separated on SDS gels and blotted onto PVDF membranes (Roche). For detection of specific proteins, the following antibodies were used: anti-PRPF8 antibody (abcam, ab79237), anti-SON antibody (Sigma HPA023535), anti-PSPC1 antibody (Abnova PAB23359), anti-SNRNP40 antibody (Abnova PAB21803) and anti-actin antibody (Cell signaling, 4967L).

Quantitative RT-PCR

Total RNA was isolated using the RNeasy Mini Kit (Qiagen). cDNA was synthesized using the TaqMan reverse transcription reagents kit (Applied Biosystems), and real-time PCR was carried out using the SYBR-Green PCR master mix (Applied Biosystems). Samples were analyzed in quadruplicates. Data shown represent mean ± SEM. Primers used were: GAPDH-forward CCACCCATGGCAAATTCC GAPDH-reverse TGGGATTTCCATTGATGACAAG CREB1-forward CAATGGGCAGACAGTTCAAG CREB1-intron-reverse GTTCTCTCCAAATCTAGGACC CREB1-exon-reverse TTCGCTTTTGGGAATCAGTT. *p* Values are the result of a factorial ANOVA determining the knock-down or genotype effect, correcting for *CREB1* exon expression, and a confounding effect of the qRT-PCR experiment.

Human postmortem brain samples

Human brain tissue was collected and stored as previously described [37]. Tissue was obtained with the families' full consent and with the approval of the Leiden University Medical Center institutional Ethics Committee. The experiments conformed to the principles set out in the WMA Declaration of Helsinki and the Department of Health and Human Services Belmont Report. Detailed information about patients is given in Table 1.

Table 1. Clinical features of brain tissue donors

ID	Sex	Age	CAG repeat	PMD
C1	M	42	–	14
C2	M	41	–	16
C3	M	89	–	19
C4	M	48	–	–
C5	F	78	–	–
C6	F	89	–	–
HD1	M	41	19/39	11
HD2	M	40	18/51	15
HD3	F	67	15/42	9
HD4	M	75	19/43	3
HD5	F	53	21/47	12
HD6	F	57	23/43	–
HD7	M	62	20/44	–
HD8	M	48	21/45	–

M, male; F, female; PMD, post-mortal delay.

Drosophila genetics

The GMR-Gal4 stock was kindly provided by P. Meier (ICR, London); UAS-flag-Prp8 stock was a gift from M. Uhlirova, University of Cologne, Germany [38]; and UAS-HttEx1Q97 was obtained from Bloomington stock center (No. 68417). Flies were raised on standard fly medium and crossed at 25 °C. Progenies were moved to 27 °C at day 3.

Supplementary data to this article can be found online at https://doi.org/10.1016/j.jmb.2019.01.034.

CRediT authorship contribution statement

Judith Schilling: Conceptualization, Data curation, Formal analysis, Investigation, Supervision, Writing - original draft, Writing - review & editing. **Meike Broemer:** Conceptualization, Data curation, Formal analysis, Investigation, Supervision, Writing - review & editing. **Ilian Atanassov:** Formal analysis, Writing - review & editing. **Yvonne Duernberger:** Data curation, Investigation, Writing - review & editing. **Ina Vorberg:** Methodology, Resources, Writing - review & editing. **Christoph Dieterich:** Formal analysis, Writing - review & editing. **Alina Dagane:** Data curation, Formal analysis, Investigation, Writing - review & editing. **Gunnar Dittmar:** Methodology, Resources, Writing - review & editing. **Erich Wanker:** Methodology, Resources, Writing - review & editing. **Willeke van Roon-Mom:** Methodology, Resources, Writing - review & editing. **Jennifer Winter:** Conceptualization, Data curation, Formal analysis, Investigation, Supervision, Writing - review & editing. **Sybille Krauß:** Conceptualization, Supervision, Writing - original draft, Writing - review & editing.

Acknowledgment

We thank Dan Ehninger and Daniele Bano for careful review of the manuscript.

Conflict of Interest: The authors declare no competing interests.

Received 24 October 2018;
Received in revised form 21 January 2019;
Accepted 24 January 2019
Available online 31 January 2019

Keywords:
neurodegeneration;
RNA-binding proteins;
CAG repeat RNA;
spliceosome;
polyglutamine disease

Abbreviations used:
HD, Huntington's disease; pre-mRNA, precursor messenger RNA; snRNP, small nuclear ribonucleoprotein.

References

[1] T.V. Strong, D.A. Tagle, J.M. Valdes, L.W. Elmer, K. Boehm, M. Swaroop, et al., Widespread expression of the human and rat Huntington's disease gene in brain and nonneural tissues, Nat. Genet. 5 (1993) 259–265.

[2] J.K. Cooper, G. Schilling, M.F. Peters, W.J. Herring, A.H. Sharp, Z. Kaminsky, et al., Truncated N-terminal fragments of huntingtin with expanded glutamine repeats form nuclear and cytoplasmic aggregates in cell culture, Hum. Mol. Genet. 7 (1998) 783–790.

[3] F. Saudou, S. Finkbeiner, D. Devys, M.E. Greenberg, Huntingtin acts in the nucleus to induce apoptosis but death does not correlate with the formation of intranuclear inclusions, Cell 95 (1998) 55–66.

[4] S. Zheng, E.B. Clabough, S. Sarkar, M. Futter, D.C. Rubinsztein, S.O. Zeitlin, Deletion of the huntingtin polyglutamine stretch enhances neuronal autophagy and longevity in mice, PLoS Genet. 6 (2010), e1000838.

[5] A.K. Thakur, M. Jayaraman, R. Mishra, M. Thakur, V.M. Chellgren, I.J. Byeon, et al., Polyglutamine disruption of the huntingtin exon 1 N terminus triggers a complex aggregation mechanism, Nat. Struct. Mol. Biol. 16 (2009) 380–389.

[6] T. Zuchner, P. Brundin, Mutant huntingtin can paradoxically protect neurons from death, Cell Death Differ. 15 (2008) 435–442.

[7] L.B. Li, Z. Yu, X. Teng, N.M. Bonini, RNA toxicity is a component of ataxin-3 degeneration in *Drosophila*, Nature 453 (2008) 1107–1111.

[8] R. Nalavade, N. Griesche, D.P. Ryan, S. Hildebrand, S. Krauss, Mechanisms of RNA-induced toxicity in CAG repeat disorders, Cell Death Dis. 4 (2013) e752.

[9] M. de Mezer, M. Wojciechowska, M. Napierala, K. Sobczak, W.J. Krzyzosiak, Mutant CAG repeats of huntingtin transcript fold into hairpins, form nuclear foci and are targets for RNA interference, Nucleic Acids Res. 39 (9) (2011) 3852–3863.

[10] S. Busan, K.M. Weeks, Role of context in RNA structure: flanking sequences reconfigure CAG motif folding in huntingtin exon 1 transcripts, Biochemistry 52 (2013) 8219–8225.

[11] J. Schilling, N. Griesche, S. Krauß, Mechanisms of RNA-induced toxicity in diseases characterised by CAG repeat expansions, eLS John Wiley & Sons, Ltd, Chichester, 2016.

[12] A. Mykowska, K. Sobczak, M. Wojciechowska, P. Kozlowski, W.J. Krzyzosiak, CAG repeats mimic CUG repeats in the misregulation of alternative splicing, Nucleic Acids Res. 39 (2011) 8938–8951.

[13] M. Banez-Coronel, S. Porta, B. Kagerbauer, E. Mateu-Huertas, L. Pantano, I. Ferrer, et al., A pathogenic mechanism in Huntington's disease involves small CAG-repeated RNAs with neurotoxic activity, PLoS Genet. 8 (2012), e1002481.

[14] S. Krauss, N. Griesche, E. Jastrzebska, C. Chen, D. Rutschow, C. Achmuller, et al., Translation of HTT mRNA with expanded CAG repeats is regulated by the MID1–PP2A protein complex, Nat. Commun. 4 (2013) 1511.

[15] A.G. Matera, Z. Wang, A day in the life of the spliceosome, Nat. Rev. Mol. Cell Biol. 15 (2014) 108–121.

[16] M.C. Wahl, C.L. Will, R. Luhrmann, The spliceosome: design principles of a dynamic RNP machine, Cell 136 (2009) 701–718.

[17] K. Sathasivam, A. Neueder, T.A. Gipson, C. Landles, A.C. Benjamin, M.K. Bondulich, et al., Aberrant splicing of HTT generates the pathogenic exon 1 protein in Huntington disease, Proc. Natl. Acad. Sci. U. S. A. 110 (2013) 2366–2370.

[18] S.H. Vo, M. Butzlaff, S.K. Pru, R.A. Ni Charthaigh, P. Karsten, A. Lankes, et al., Large-scale screen for modifiers of ataxin-3-derived polyglutamine-induced toxicity in *Drosophila*, PLoS One 7 (2012), e47452.

[19] G. Xu, T. Li, J. Chen, C. Li, H. Zhao, C. Yao, et al., Autosomal dominant retinitis pigmentosa-associated gene PRPF8 is essential for hypoxia-induced mitophagy through regulating ULK1 mRNA splicing, Autophagy 14 (2018) 1818–1830.

[20] V.O. Wickramasinghe, M. Gonzalez-Porta, D. Perera, A.R. Bartolozzi, C.R. Sibley, M. Hallegger, et al., Regulation of constitutive and alternative mRNA splicing across the human transcriptome by PRPF8 is determined by 5′ splice site strength, Genome Biol. 16 (2015) 201.

[21] T. Mantamadiotis, T. Lemberger, S.C. Bleckmann, H. Kern, O. Kretz, A. Martin Villalba, et al., Disruption of CREB function in brain leads to neurodegeneration, Nat. Genet. 31 (2002) 47–54.

[22] J. Lee, C.H. Kim, D.K. Simon, L.R. Aminova, A.Y. Andreyev, Y.E. Kushnareva, et al., Mitochondrial cyclic AMP response element-binding protein (CREB) mediates mitochondrial gene expression and neuronal survival, J. Biol. Chem. 280 (2005) 40398–40401.

[23] A.C. McCourt, J. Parker, E. Silajdzic, S. Haider, H. Sethi, S.J. Tabrizi, et al., Analysis of white adipose tissue gene expression reveals CREB1 pathway altered in Huntington's disease, J. Huntingtons Dis. 4 (2015) 371–382.

[24] H. Jeong, D.E. Cohen, L. Cui, A. Supinski, J.N. Savas, J.R. Mazzulli, et al., Sirt1 mediates neuroprotection from mutant huntingtin by activation of the TORC1 and CREB transcriptional pathway, Nat. Med. 18 (2011) 159–165.

[25] G.R. Jackson, I. Salecker, X. Dong, X. Yao, N. Arnheim, P.W. Faber, et al., Polyglutamine-expanded human huntingtin transgenes induce degeneration of *Drosophila* photoreceptor neurons, Neuron 21 (1998) 633–642.

[26] A. Neueder, C. Landles, R. Ghosh, D. Howland, R.H. Myers, R.L.M. Faull, et al., The pathogenic exon 1 HTT protein is produced by incomplete splicing in Huntington's disease patients, Sci. Rep. 7 (2017) 1307.

[27] L. Lin, J.W. Park, S. Ramachandran, Y. Zhang, Y.T. Tseng, S. Shen, et al., Transcriptome sequencing reveals aberrant alternative splicing in Huntington's disease, Hum. Mol. Genet. 25 (2016) 3454–3466.

[28] T. Kanashova, O. Popp, J. Orasche, E. Karg, H. Harndorf, B. Stengel, et al., Differential proteomic analysis of mouse macrophages exposed to adsorbate-loaded heavy fuel oil derived combustion particles using an automated sample-preparation workflow, Anal. Bioanal. Chem. 407 (2015) 5965–5976.

[29] J. Rappsilber, M. Mann, Y. Ishihama, Protocol for micro-purification, enrichment, pre-fractionation and storage of peptides for proteomics using StageTips, Nat. Protoc. 2 (2007) 1896–1906.

[30] J. Cox, M. Mann, MaxQuant enables high peptide identification rates, individualized p.p.b.-range mass accuracies and proteome-wide protein quantification, Nat. Biotechnol. 26 (2008) 1367–1372.

[31] S. Tyanova, T. Temu, P. Sinitcyn, A. Carlson, M.Y. Hein, T. Geiger, et al., The Perseus computational platform for comprehensive analysis of (prote)omics data, Nat. Methods 13 (2016) 731–740.

[32] R Core Team, R: A Language and Environment for Statistical Computing, R Foundation for Statistical Computing, Vienna, Austria, 2016.

[33] M.E. Ritchie, B. Phipson, D. Wu, Y. Hu, C.W. Law, W. Shi, et al., limma powers differential expression analyses for RNA-sequencing and microarray studies, Nucleic Acids Res. 43 (2015) e47.

[34] J. Chen, E.E. Bardes, B.J. Aronow, A.G. Jegga, ToppGene suite for gene list enrichment analysis and candidate gene prioritization, Nucleic Acids Res. 37 (2009) W305–W311.

[35] I. Cvitkovic, M.S. Jurica, Spliceosome database: a tool for tracking components of the spliceosome, Nucleic Acids Res. 41 (2013) D132–D141.

[36] G. Yeo, C.B. Burge, Maximum entropy modeling of short sequence motifs with applications to RNA splicing signals, J. Comput. Biol. 11 (2004) 377–394.

[37] H.J. Waldvogel, J.Y. Bullock, B.J. Synek, M.A. Curtis, W.M. van Roon-Mom, R.L. Faull, The collection and processing of human brain tissue for research, Cell Tissue Bank. 9 (2008) 169–179.

[38] A.K. Claudius, P. Romani, T. Lamkemeyer, M. Jindra, M. Uhlirova, Unexpected role of the steroid-deficiency protein ecdysoneless in pre-mRNA splicing, PLoS Genet. 10 (2014), e1004287.